Institution of MECHANICAL ENGINEERS
Journal of MECHANICAL ENGINEERING SCIENCE

Original Article

Proc IMechE Part C:
J Mechanical Engineering Science
2014, Vol. 228(14) 2469–2482

DOI: 10.1177/0954406213519614
pic.sagepub.com
SAGE

Bending and contact fatigue strength of innovative steels for large gears

Carlo Gorla, Francesco Rosa, Edoardo Conrado and Horacio Albertini

Abstract

Large gears for wind turbine gearboxes require high performances and cost-effective manufacturing processes. Heat distortion in the heat treatment phase and the consequent large grinding stock are responsible for high manufacturing costs due to reduced productivity. A research project aimed at the identification of new materials, manufacturing and heat treatment processes has been performed. Air quenchable alloy steels, combined with a specifically developed case hardening and heat treatment process, have been identified as an interesting solution, both from the point of view of cost effectiveness, thanks to reduced distortions and grinding stock, and for the environmental sustainability. The research project has been completed by the manufacturing of a full-scale gear, on which the whole process has been validated. Nevertheless, in order to judge the applicability of these steels to large gears, data from specific tests on the performances against typical gear failure modes, like bending and contact fatigue, are necessary as well. Single tooth fatigue bending tests and disc-on-disc contact fatigue tests have therefore been performed on two innovative materials, respectively, a high hardenability steel and a bainitic structure steel, and on a reference traditional case hardening steel. The results of these tests, which provide useful data for gear designers, are presented and discussed in this paper.

Keywords

Gears, bending fatigue, micropitting, gear steels, wind turbine

Date received: 21 May 2013; accepted: 13 December 2013

Introduction

Large gears for wind turbine gearboxes in terms of performance, reliability, quality and cost-effectiveness represent a challenge for manufacturing processes and material selection. The traditional production methods are proving to be inadequate for a cost-effective mass production of large and high quality gears, due to the costs of the final grinding step. In particular, as a consequence of the distortions of the heat treatment phase, the large stock removal of the final finishing grinding reduces the productivity of the process thus increasing its costs.

On one side, manufacturers of grinding machines are actively working to improve the productivity of the grinding process itself by introducing new approaches, machines and tools. On the other side, it is quite evident that also a reduction of heat treatment distortions by means of the selection of new materials and heat treatments can represent a valid approach to cut grinding costs and manufacturing time.

A research project, named XL-GEARS, has been carried out with the aim of identifying alternative gear manufacturing processes and materials that could reduce the heat treatment distortions in order to reduce the stock removal of the final grinding operation. In particular, the possibility to reduce heat treatment distortion with application to large gears of wind turbine gearboxes of materials suitable for air quenching has been investigated. Air quenching also represents a relevant improvement in terms of environmental sustainability of the manufacturing process with respect to the more traditional oil quenching.

Many aspects have been approached in the XL-GEARS project, as the material selection, the development of the whole manufacturing process and of the heat treatment, including the necessary metallurgical test aimed at the verification of the properties obtained, both on representative specimen and on a final full-scale prototype that has been manufactured. A phase of the research has also been devoted to the investigation of the possible benefits

Dipartimento di Meccanica, Politecnico di Milano, Milano, Italy

Corresponding author:
Edoardo Conrado, Dipartimento di Meccanica, Politecnico di Milano, via La Masa 1, 20156 Milano, Italy.
Email: edoardo.conrado@polimi.it

of coatings. Concerning material selection, two alternatives have been identified, the first characterized by a high jominy hardenability, having the commercial name of Jomasco, and the second by a bainitic structure, named Metasco, both suitable for air quenching.

The basic mechanical and metallurgical properties of these materials allow only a preliminary evaluation of their suitability for gear applications; specific tests referring to typical failure modes of gears are required for a reliable judgement. An important phase of the research that is the main object of the present paper has therefore been devoted to investigate the performances of the selected materials with respect to two typical gear failure modes, i.e. bending and contact fatigue. The strength properties of the new materials have then been compared with those of a traditional solution, represented by the typical and widespread in Italy case hardening steel 18NiCrMo5. The bending fatigue limits of these materials have been determined by means of single tooth fatigue (STF) tests on a mechanical resonance pulsator by means of specimens specifically designed for the present research. Since micropitting represents one of the typical surface damage phenomenon which can occur on large case hardened gears of wind turbine gearboxes, a campaign of tests on disc specimens has also been carried out to compare the contact fatigue strength of these materials. The final results of these tests, which provide material limits for bending fatigue and a comparative evaluation of the micropitting strength, are hereafter presented and discussed.

New materials

The selection of new materials for application to large gears of wind turbines was restricted to alloyed steels suitable for case hardening, and it was based on a preliminary definition of the main performances and manufacturing requirements.

Beside air hardenability, as already pointed out, the considered aspects comprise high mechanical strength; toughness, even at low temperatures and low distortion after heat treatment, in order to reduce grinding stock. It has also to be highlighted that the grinding stock reduction represents a direct benefit for the grinding time, but it also represents an advantage for the heat treatment phase, because the design case depth on the finished part can be obtained with a lower pre-grind case hardening depth, thus reducing also the carburizing time.

Other metallurgical properties have been considered, such as the absence of residual austenite after quenching and low size of the austenitic grain. Good machinability and availability on the market are other interesting aspects.

The final choice is represented by two alloy steels, produced by ASCOMETAL/LUCCHINI, belonging respectively to the class of high hardenability steels (Jomasco) and microalloyed steels (Metasco). They have been selected for their quenching behaviour: the former is characterized by high jominy hardenability while the latter, thanks to its peculiar chemical composition, has a fine bainitic structure after air quenching that enables a good mechanical resistance. These characteristics, combined with a specifically developed case hardening treatment, allow the obtainment of high surface properties on large size parts without oil quenching as expected.

The selection of the materials was based on metallurgical tests aimed to identify and optimize the heat treatment process in order to obtain the desired properties on gears of large dimensions. This part of the research is described in detail in Ref. 1 and will be the subject of a specific paper under development.

Gear designers can easily find fatigue limits for almost all materials and heat treatments commonly used in gear manufacturing in the specialized literature or in gear standards, see for example Refs. 2,3. On the other hand, new materials are continuously developed in order to increase the load-carrying capacity of gears. Several projects have been performed to investigate the influence of material and manufacturing processes.[4–7] Nevertheless, few papers present results of investigations on the above introduced materials, even though these materials exhibit very promising characteristics. In particular, only Lemaitre et al.[8] have presented the results of experimental tests directly aimed to evaluate the resistance of gears manufactured with Jomasco and Metasco steels. It is important to observe that Lemaitre et al. have used nitrided specimens, instead of the carburized and case hardened gears used in the research presented here. Even though their bending fatigue tests were not exactly representative of actual gear strengths, since they used four-point bending specimens, these tests resulted in a 15–20% increase of the 'endurance limit' with respect to the base material (42CrMo4). As a result of surface fatigue tests (performed on a twin-disc machine), Lemaitre et al. have found on Jomasco and Metasco sample surfaces some 'flakes' that they attributed to sulphurs presence. Anyhow, they did not provide any quantitative evaluation of the results of surface fatigue tests.

Bending fatigue tests

As tests with running gears are more expensive and time consuming, gear bending fatigue tests are commonly performed loading one tooth at a time. In this type of tests, commonly named STF tests, the load is applied directly to the tooth under test by means of a specifically designed anvil and reacted by another anvil in contact with another tooth. In this way, several tests can be performed on the same gear reducing specimen manufacturing time and costs. Furthermore, the applied load is accurately controlled and measured, since it is directly applied on the tooth under test. The main difference with respect to the gear

meshing conditions is the stress ratio R defined as the ratio between minimum and maximum applied load: in actual meshing this ratio is zero, while in these tests it is usually chosen equal to 0.1 (see e.g. Ref. 9), since in STF tests it is not possible to completely unload the teeth. The STF method has been adopted in this experimental campaign.

Test design and procedure

Since the scope of the bending tests was the determination of fatigue limits, the load sequences for each material, i.e. for each specimen family, were determined following the staircase approach.

Three case hardened steels were tested: 18NiCrMo5, Jomasco and Metasco. The chemical compositions of these gear steels are presented in Table 1. The run-out value was set at five million load cycles, as bending fatigue S/N diagrams for case hardened materials present typically their knee of the fatigue limit at three million load cycles.[3]

Regarding specimen geometry, due to the load limits of the available test apparatus, a test gear module smaller than those generally employed for gears of wind turbine gearboxes object of this research was used. In any case the adopted module is in the range in which the size factor (Y_X according to ISO 6336) is different from one. Taking into account the maximum load (60 kN) that can be exerted by the available testing machine, a module of 8 mm was eventually selected. The main geometrical data of the gear specimen are listed in Table 2. The test gears had an ISO Accuracy Grade equal to 6 according to the ISO standard 1328-1:1995, i.e. in the range prescribed by ISO 6336-5:2003 for bending test on gears. The average of the arithmetic mean surface roughness (Ra) measured over three teeth of each test gear at the tooth root fillet was in the range between 0.50 and 0.65 μm. All these test gears were case hardened and ground. Figure 1 shows the microhardness profiles obtained at the tooth root for the three materials. The effective case depth measured at the tooth root after the grinding process was 1.0 mm for the 18NiCrMo5, while for the two new steels was lower: 0.8 mm for the Jomasco and 0.7 mm for the Metasco. On the contrary, the two new materials showed a higher surface hardness, for both 64 HRC, than the one of the baseline material hardness (61 HRC). The core hardness was 384 HV for the 18NiCrMo5, 330 HV for the Jomasco and 360 HV for the Metasco. The material grade for the three case-hardened steels was ML according to ISO 6336-5:2003.

The tests were performed on a mechanical resonance Schenck pulsator with an axial load capacity of 60 kN. This test bench has two load application systems, one used for the application of a static load and the other one generating a dynamic load by the rotation of an unbalanced rotor operating in the resonance range. This dynamic force was controlled by a closed-loop control system adjusting the rotational speed of the unbalanced rotor. The total force applied was measured by a U2B HBM load cell with a nominal rated force of 100 kN. These measurements during tests show that the mean load was practically constant, while the amplitude changes were less than 1.2 kN.

Figure 2 shows the schema of the configuration of the loading fixtures mounted on the testing device. One side is fixed, while the oscillating load is applied through the movable anvil. Since three teeth are comprised between the tooth under test and the tooth used to react to the load, eight tests can be performed on the 32 teeth of each toothed gear. Teeth adjacent to a tested tooth are not used, as they are subjected to stresses during the test, as well. During the present experimental campaign, two toothed wheels were used for the baseline steel and the Metasco, while three wheels were used for the Jomasco. The positioning of the gear is obtained by means of a pin inserted in the hole of the hub and in the supporting structure. Since the load applied to the gear acts along the tangent to the base circle, the axis of the holes in the supporting structure is set at a vertical distance equal to the base radius from the axis of the machine: in this way moments on the load cell are avoided and only forces act on it. The horizontal position of the pin can be adjusted by means of shims. Since the distance from the two loaded flanks along a line tangent to the base circle is the span measurement on five teeth, if the pin axis is set at a distance from the

Table 1. Chemical composition of the Jomasco and the Metasco steels along with the one of the base line material.

	Chemical composition by wt%						
Steel grade	C	Si	Mn	Cr	Mo	Ni	V
18NiCrMo5	0.18	0.23	0.65	0.93	0.19	0.89	–
Jomasco®	0.24	0.29	1.34	1.21	0.25	0.24	–
Metasco®	0.24	0.71	1.63	0.78	0.07	0.10	0.20

Table 2. Main data of gear specimen for bending tests.

Parameter	Symbol	Unit	Value
Module	m	mm	8
No. of teeth	Z	/	32
Pressure angle	A	deg	20
Face width	B	mm	20
Addendum modification coefficient	X	/	0.226
Basic rack	ISO 53.2 –B		
Tip diameter	d_a	mm	276

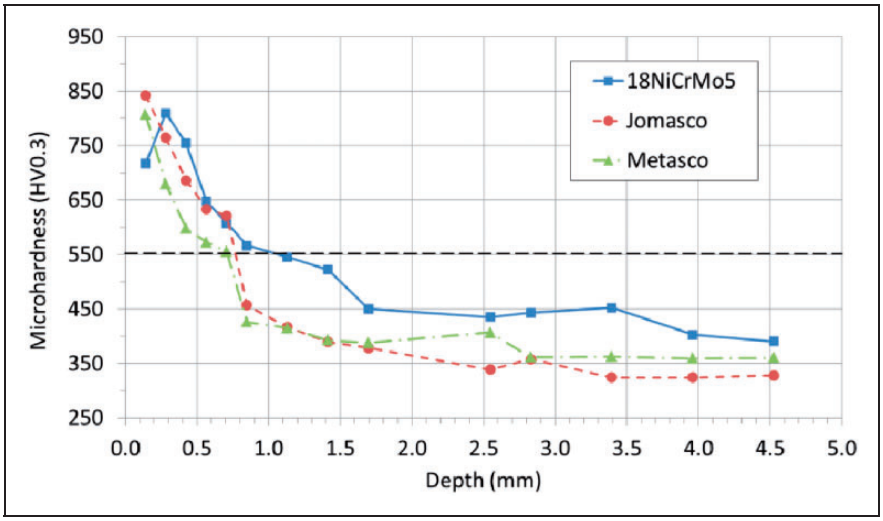

Figure 1. Microhardness profile measured in the mid face at the tooth root for the three case-hardened steels.

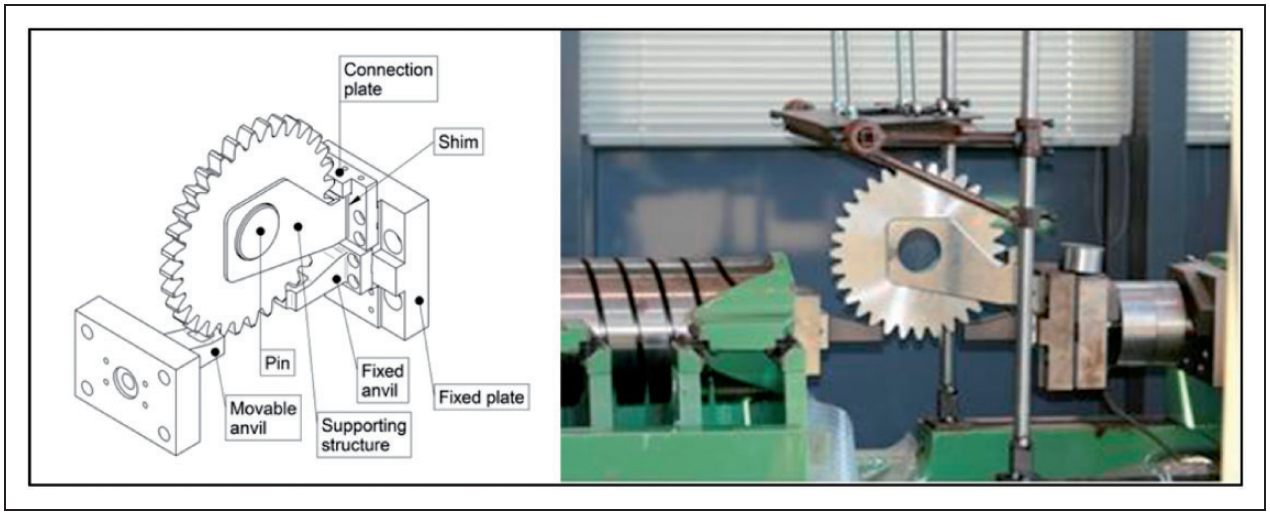

Figure 2. Bending fatigue test apparatus: on the left a 3D schema and part nomenclature; on the right gear mounted on the test rig.

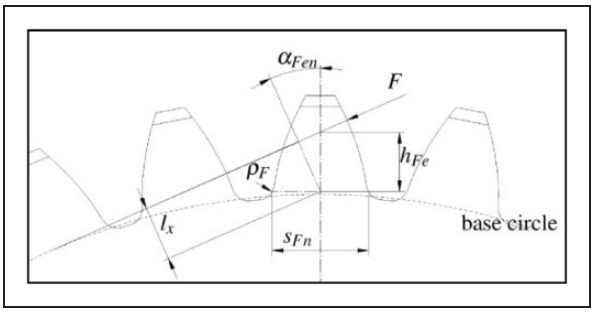

Figure 3. Main geometrical data for bending root stress calculation according to ISO 6336:2006.

fixed anvil (distance X, see Figure 4) equal to half of this span measurement (W_5), a symmetric loading condition is obtained and the root stress is the same on the two teeth. Different root stresses can be obtained with non-symmetric positions ($X \neq W_5/2$). In order to maximize the obtainable root stress on one of the two teeth, a non-symmetric condition has been used.

As a concluding remark, it is worth noting that the pin is used only in the setting phase and is then removed; therefore, during the tests, the gear is supported only by the anvils, contrarily to what happens in other well-known applications (see e.g. Refs. 9,10), because the presence of the pin is incompatible with a resonance machine, which does not stop immediately at the tooth breakage, and would require an hydraulic testing machine.

Bending stress calculation

The load–stress relationship discussed in this section has been derived to obtain results directly comparable with values reported in international standards.[3] First, the general formulation presented in Ref. 11 is

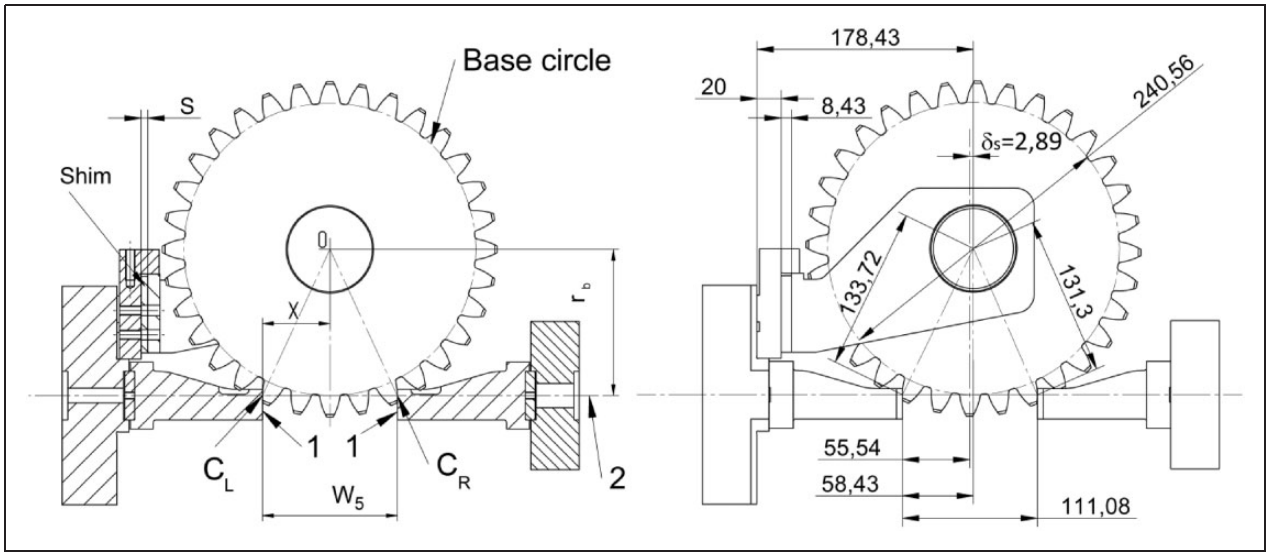

Figure 4. Main dimensions of the rig and of the gear used to determine load application point.

introduced and examined in order to derive the load–stress relationship taking into account the actual load application point. Finally, it will be shown how to derive fatigue limits directly comparable with the nominal stress number for bending as defined in Ref. 11, i.e. the bending stress limit defined by ISO in standardized conditions (material, heat treatment and surface roughness of root fillet).

Applied load and bending stress according to ISO 6336. In order to make the experimental results comparable with standard data, the relationship between applied force and root bending stress has been developed by adapting the method B of ISO 6336-3:2006 to the previously mentioned non-symmetric loading conditions. According to ISO 6336-3:2006,[11] the tooth root stress can be determined by means of the following equation

$$\sigma_F = \frac{F_t}{b \cdot m} \cdot \left(Y_F \cdot Y_S \cdot Y_\beta \cdot Y_B \cdot Y_{DT}\right) \cdot \left(K_A \cdot K_V \cdot K_{F\alpha} \cdot K_{F\beta}\right) \tag{1}$$

According to their definitions, the only factors that are different from one in the present condition are those remaining in the following equation

$$\sigma_F = \frac{F_t}{b \cdot m} \cdot Y_F \cdot Y_S$$

where F_t is the tangential force (i.e. the 'transverse load tangential to the reference cylinder'), m the module and b the face width. The tangential load is related to the applied load F by the following equation

$$F_t = F \cdot cos(\alpha)$$

where $\alpha = 20^\circ$ is the pressure angle at the reference diameter. The form factor Y_F for a spur gear is defined by the following equation that uses symbols illustrated in Figure 3

$$Y_F = \frac{6 \cdot \frac{h_{Fe}}{m} \cdot \cos(\alpha_{Fen})}{\left(\frac{s_{Fn}}{m}\right)^2 \cdot \cos(\alpha)}$$

and the stress correction factor Y_S is defined by the following equation

$$Y_S = (1.2 + 0.13 \cdot L) \cdot q_S^{L/(1.21 \cdot L + 2.3)}$$

where $L = S_{Fn}/h_{Fe}$ and $q_S = s_{Fn}/(2 \cdot \rho_F)$. The root curvature radius (ρ_F) and the tooth root normal chord (S_{Fn}) have been determined by means of the procedure described in Ref. 12. The other geometrical quantities, i.e. the bending moment arm (h_{Fe}) and the angle (α_{Fen}) between the applied force and the normal to the tooth axis, have been calculated according to the ISO method B[11] taking into account that the load is applied at the radial distance determined in the next subsection.

Table 3 presents the results of the calculations. In particular, the last row of this table shows the root bending stress corresponding to a 1 kN load.

Loading radius calculation. Let C_R and C_L be the points where the planar faces (1) of the movable and the fixed anvils are in contact with the corresponding tooth flanks as represented in Figure 4 and let S_0 be the shim thickness corresponding to the symmetric condition. If a shim with a different thickness is used, the two contact radii differ. If a shim with a thickness S equal to $S_0 + \delta_s$ is used (i.e. distance X is equal to $W_5/2 + \delta_s$), the gear moves horizontally to the right, and rotates clockwise. As a result, the radius of contact point C_L is increased. Thus, in this asymmetric condition, one of the loaded tooth is stressed more than the other one since the load is applied at a higher

radial distance from the toothed wheel centre that, on the basis of the geometrical quantities shown in Figure 4, can be calculated as follows

$$R_L = \overline{OC_L} = \sqrt[2]{(W_5/2 + \delta_S)^2 + r_b^2}$$

This is the solution that, as already mentioned, has been adopted during all the tests, in order to obtain an adequate bending stress, without reaching the operative limits of the testing machine. Practically, the thickness variation δ_s of the adopted shim is equal to 2.89 mm. The resulting thickness ensures also an adequate clearance between the tip of the right tooth and the corresponding anvil.

Experimental test results and failure analyses

In this section the results of the fatigue tests are presented and discussed. Table 4 presents the results of the bending tests on the baseline material, the 18NiCrMo5 steel. On the failed teeth of the two gears of this family, Scanning Electron Microscope (SEM) analysis was performed. Even if small inclusions were found in some cases, it was not generally possible to associate them to an origin of tooth failure. As an example, Figure 5 shows a defect found near the loaded edge of the tooth failed during test no. 15 at 52 kN. Tables 5 and 6 present the results of the tests performed, respectively, on the Jomasco and Metasco specimens. The analyses of some of the failed teeth showed the presence of sulphur inclusions containing also manganese and molybdenum, as shown, for example, in Figures 5 and 6 for the Jomasco specimens and in Figure 7 for the Metasco specimens.

The statistical analysis of the results of the bending fatigue tests was performed following the Dixon and Mood approach.[13] The result is the fatigue limit (at 50% probability) of the tested specimens and their standard deviation. In this section, the results are still presented in terms of applied forces; their conversion in bending stresses is discussed in the next section, where a comparison with ISO standard values is also presented.

For each test, the applied loads have been sorted in levels (i), and then the number of occurrences at each load level of the less frequent event is annotated (n_i). Finally, the rightmost two columns of Tables 4, 5 and 6 are computed.

On the basis of these coefficients, it is possible to determine the fatigue limit (μ_D) and its standard deviation (σ_D) by means of the following equations

$$\mu_D = F_0 + d \cdot \left(\frac{A}{N} \pm \frac{1}{2}\right)$$

$$\sigma_D = \begin{cases} 1.62 \cdot d \cdot \left(\frac{N \cdot B - A^2}{N^2} + 0.029\right) & \text{if } \frac{N \cdot B - A^2}{N^2} \geqslant 0.3 \\ 0.53 \cdot d & \text{if } \frac{N \cdot B - A^2}{N^2} < 0.3 \end{cases}$$

where $d = 2$ kN is the step between two consecutive load levels and F_0 is the lower load at which the less

Table 3. Factors for the tooth root strength calculation according to ISO 6336-3:2006.

Parameter	Unit	Value
h_F	mm	10.811
l_x	mm	9.886
$\alpha_{F_{en}}$	deg	23.8769
s_{F_n}	mm	17.357
ρ_F	mm	3.383
q_s	/	2.565
L	/	1.605
Y_F	/	1.676
Y_S	/	2.012
σ_{F_0}/F	MPa/kN	19.807

Table 4. Results of the bending tests on the 18NiCrMo5 specimens.

18NiCrMo5																						
F	Test number																					
(kN)	1	2	3	4	5	6	7	8	9	10	11	12	13	14	15	16	x	o	i	n_i	$i*n_i$	i^2*n_i
60	x																1	0	6	0	0	0
58		x															1	0	5	0	0	0
56			x														1	0	4	0	0	0
54				x													1	0	3	0	0	0
52					x		x		x		x				x		5	0	2	0	0	0
50						o		o		o		x		o		o	1	5	1	5	5	5
48													o				0	1	0	1	0	0
F = nominal value of the maximum load															Total		10	6		6	5	5
																				N	A	B

x = failure; o = runout; $N = \Sigma_i(i)$; $A = \Sigma_i(i*n_i)$; $B = \Sigma_i(i^2*n_i)$.

frequent event occurred; the positive sign is used if the run-out is the less frequent event, otherwise the negative sign is used.

Applying these equations to baseline gear test results (see Table 4), a fatigue limit equal to 50.7 kN, with a 1.1 kN standard deviation has been obtained.

Table 5 has been built on the basis of the experimental results of Jomasco specimens, taking into account that the failure is the less frequent event. A 53.8 kN fatigue limit with a standard deviation equal to 2.2 kN has therefore been obtained. Also for the Jomasco gears, the step d is comprised in the allowable range (i.e. between the half and the double of the standard deviation), even if the dispersion of the results is greater than in the baseline gears.

On the basis of the test results on Metasco gears, Table 6 has been built. As a result, a fatigue limit equal to 48.4 kN and a standard deviation equal to 3.5 kN were obtained. It is worth noting that load step is sufficiently close to the standard deviation. Table 7 summarizes the results at 50% failure probability and also those calculated at 1%, to be comparable with the limits given by the standards.[3] Even taking into account of the statistical nature of the results, it can be at least concluded that Jomasco bending fatigue limit is comparable with the limit of the baseline solution, while Metasco results in a slightly lower limit.

Definition of fatigue limit according to ISO 6336. According to ISO 6336-3:2006, the bending fatigue resistance assessment is satisfied if

$$\sigma_{FG}/\sigma_F > s_{Fmin} \tag{2}$$

where s_{Fmin} is the minimum acceptable safety factor against tooth breakage, and

$$\sigma_{FG} = \sigma_{Flim} \cdot Y_{ST} \cdot Y_{NT} \cdot Y_{\delta relT} \cdot Y_{RrelT} \cdot Y_X \tag{3}$$

This expression relates 'the nominal stress number (bending) from reference test gears' (see ISO 6336-5) (σ_{Flim}) to the tooth root stress limit (σ_{FG}) of the gear under exam (i.e. the tested gears) by means of five coefficients listed in Table 8 (definitions are taken from ISO 6336-3:2006 Clause 5.3.2). The values of Y_X, $Y_{\delta rel\tau}$, $Y_{Rrel\tau}$ have been determined according to the procedure described in Clause 15, 13 and 14 of ISO 6336-3:2006.

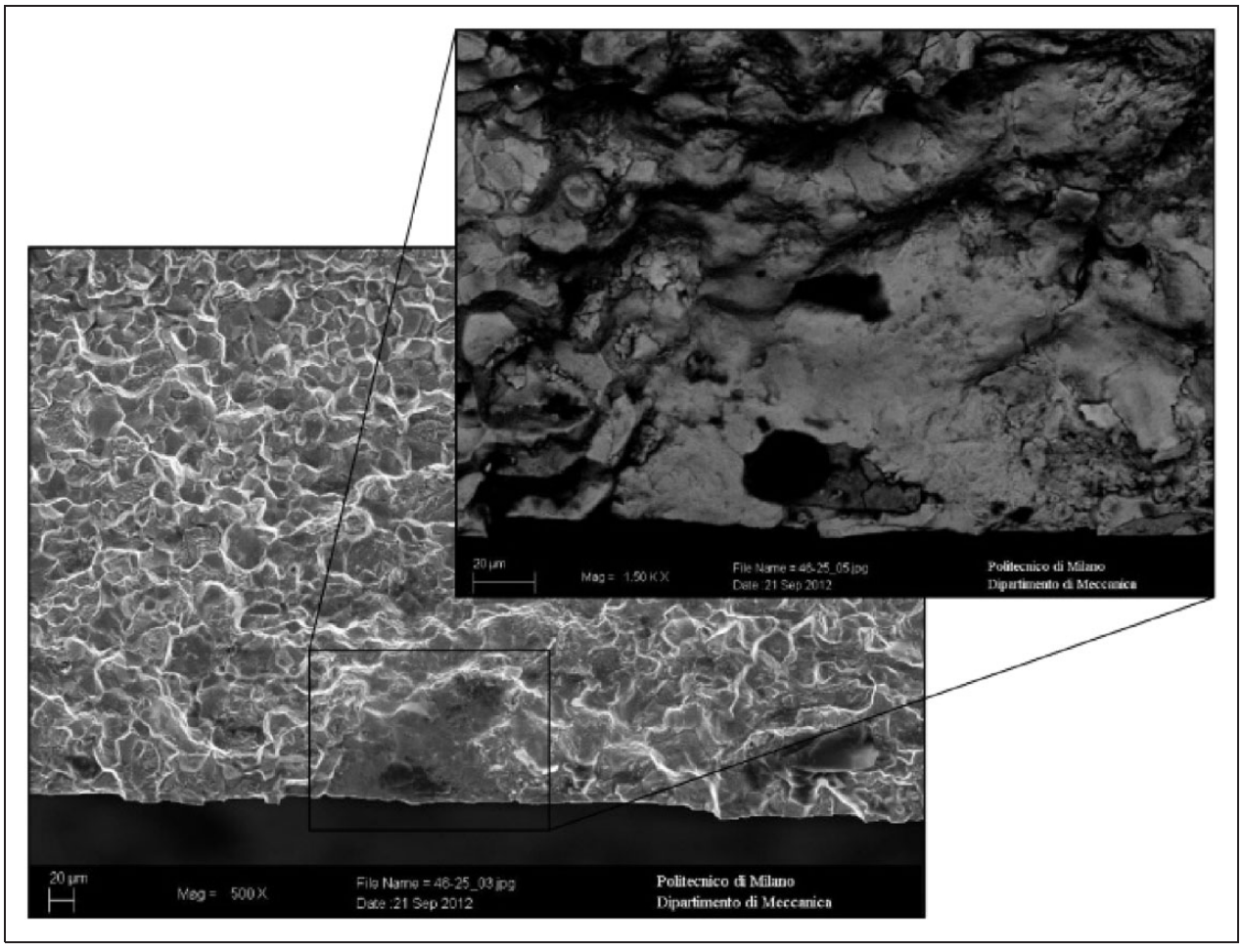

Figure 5. SEM microphotography of a defect discovered in fracture surface of the tooth failed during test no. 15 at 52 kN on the 18NiCrMo5. This defect was close to the edge of the flank where load was applied.

Table 5. Results of the bending tests on the Jomasco specimens.

Jomasco																												
F	Test number																											
(kN)	1	2	3	4	5	6	7	8	9	10	11	12	13	14	15	16	17	18	19	20	21	22	23	x	o	i	n_i	$i*n_i$	i^2*n_i
56					x		x						x		x				x		x		o	6	1	2	6	12	24
54				o		o		x				o		o		x		o		o		o		2	7	1	2	2	2
52	x		o						x		o						o							2	3	0	2	0	0
50		o								o														0	2	-	-	-	-
F = nominal value of the maximum load																						Total		10	13		10	14	26
																											N	A	B

x = failure; o = runout; $N = \Sigma_i(i)$; $A = \Sigma_i(i*n_i)$; $B = \Sigma_i(i^2*n_i)$.

Table 6. Results of the bending tests on the Metasco specimens.

Metasco																							
F	Test number																						
(kN)	1	2	3	4	5	6	7	8	9	10	11	12	13	14	15	16	17	x	o	i	n_i	$i*n_i$	i^2*n_i
52	x								x		x							3	0	4	0	0	0
50		x				x		o		o		x						3	2	3	2	6	18
48			x		o		o						x				x	3	2	2	2	4	8
46				o										x		o		1	2	1	2	2	2
44															o			0	1	0	1	0	0
F = nominal value of the maximum load																	Total	10	7		7	12	28
																					N	A	B

x = failure; o = runout. $N = \Sigma_i(i)$; $A = \Sigma_i(i*n_i)$; $B = \Sigma_i(i^2*n_i)$.

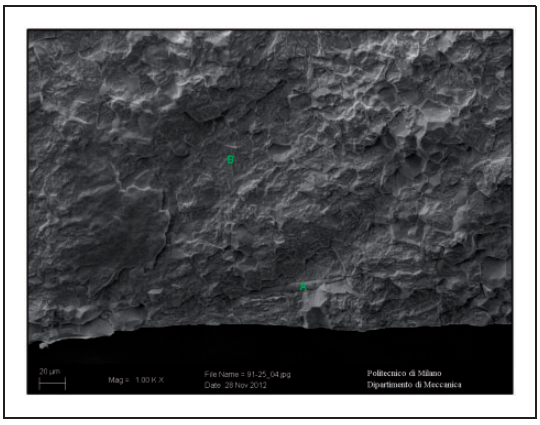

Figure 6. SEM microphotography of an inclusion discovered in the fracture surface of the tooth failed during test no. 7 at 56 kN on the Jomasco. This inclusion was near to the loaded flank.

Assuming that s_{Fmin} is equal to 1 (since the final aim consists in determining the fatigue limit), by combining equations (1) to (3) the following expression of the 'the nominal stress number (bending) from reference test gears' (see ISO 6336-5) (σ_{Flim}) can be obtained

$$\sigma_{Flim} = \left(\frac{F \cdot cos(\alpha)}{b \cdot m}\right) \cdot \left(K_A \cdot K_V \cdot K_{F\alpha} \cdot K_{F\beta}\right) \cdot \frac{Y_F \cdot Y_S \cdot Y_\beta \cdot Y_B \cdot Y_{DT}}{Y_{ST} \cdot Y_{NT} \cdot Y_{\delta relT} \cdot Y_{RrelT} \cdot Y_X}$$

By replacing F with the above determined fatigue limits ($\mu_{(99\,\%)}$), the values of the 'the nominal stress number (bending)' listed in rightmost column of Table 7 have been obtained. These results are in the typical range of the standardized values of case-hardened wrought steels.

Micropitting

Micropitting (or grey staining) is recognized to be a type of surface fatigue damage of gears. It has become a major concern in certain classes of industrial gear applications, such as wind turbine gearboxes, as a consequence of the increasing utilization of surface

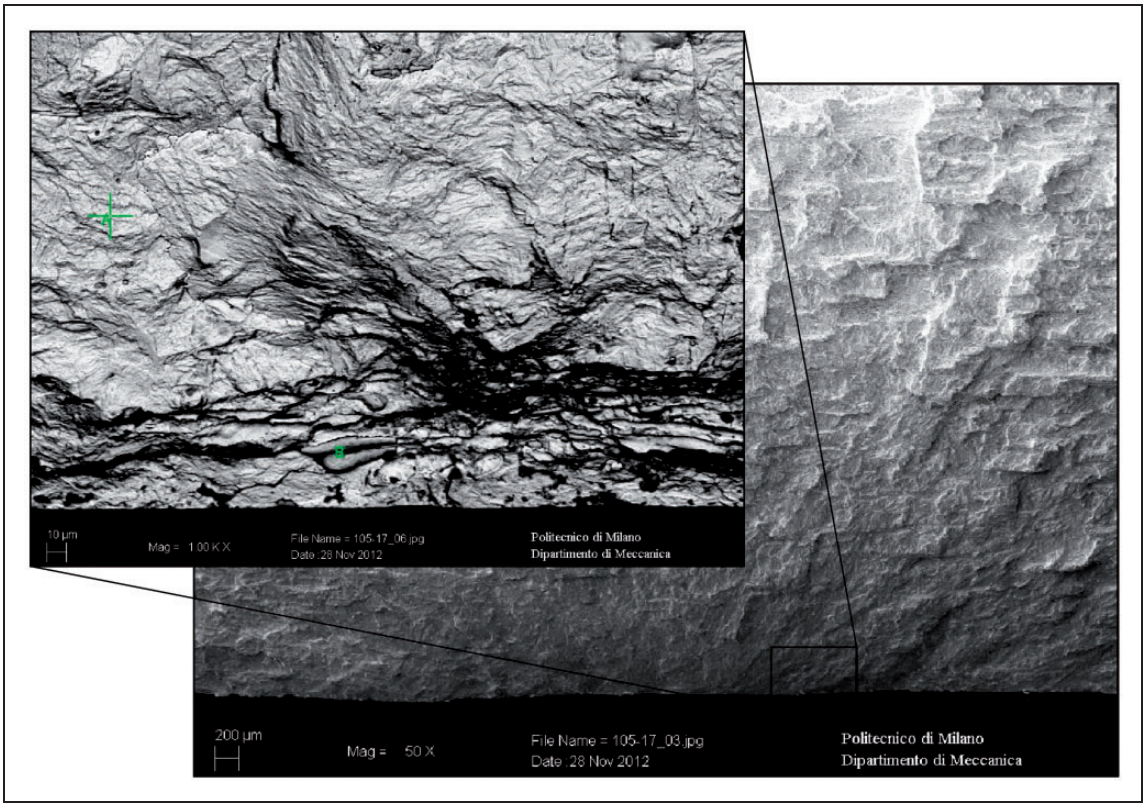

Figure 7. SEM microphotography of an inclusion found in the tooth failed during test no. 6 at 50 kN. In position B, 35.7% of weight is sulphur, 62.23% of manganese and 2.07% of iron. This inclusion was near to the load application flank.

Table 7. Results of the bending tests.

Material	μ_D (kN)	σ_D (kN)	μ (99%)[a] (kN)	$\sigma_{F\,\mathrm{lim}}$ (MPa)
18NiCrMo5	50.7	1.1	48.2	514
Jomasco	53.8	2.2	48.8	520
Metasco	48.4	3.5	40.2	429

[a] $\mu_{(99\%)} = \mu_D - 2.326355\ \sigma_D$.

Table 8. Factors according to ISO 6336.

Factor	Value	Description
Y_{ST}	2	The stress correction factor
Y_{NT}	1	Life factor for tooth root stress
$Y_{\delta_{relT}}$	1.001	Relative notch sensitivity factor
$Y_{R_{relT}}$	0.957	Relative surface factor
Y_X	0.97	Size factor

hardened gears (case carburized, nitrided), of steels of improved quality and high cleanliness and of lubricants with sophisticated additive packages that enable gears to work in non-favourable lubrication conditions without the occurrence of other types of damages. The micropitting damage occurrence is strongly influenced by the tribological system consisting of the tooth flank surfaces and the lubricant. The lubricant, its base oil properties and additive packages, as well as the surface roughness are the main parameters commonly considered for an improvement of the micropitting load-carrying capacity of gears. Nevertheless, also the material strength plays a major role in determining the micropitting load-carrying capacity of gears, and increases as large as 1:3 (see e.g. Ref. 14) can be achieved using different gear materials. For this reason, the micropitting strength is an important parameter to be taken into account in the selection of new gear materials.

The micropitting strength of gear materials is commonly investigated by means of bench tests on gears or on discs.

In gear tests, materials, manufacturing processes, heat treatments and micro and macro geometries of gear specimens, as well as the test conditions, can be selected in order to obtain results representative of real gear applications. Tribological, kinematic and operating conditions close to real gear applications can be reproduced in these tests that are often performed on back-to-back gear test rigs like the Forschungsstelle für Zahnräder und Getriebebau (FZG) and the Ryder ones. As a result, these tests give reliable results that can be used in conjunction with standardized calculation methods (see e.g. Ref. 14) in order to predict the micropitting load-carrying capacity of actual gears. Unfortunately this type of

tests is quite expensive and time consuming due to the complexity of the required test apparatus.

On the contrary, tests on discs require less complex test benches and test specimens. Nevertheless, they cannot reproduce the variation of the tribological contact conditions of gears since they can simulate only the kinematic conditions occurring in a single point along the path of contact of a gear pair. For this reason, investigations about rolling contact fatigue of gear steels conducted on discs may not show a good absolute correlation with results of gear tests, but, generally, have a good relative correlation with them.[15,16]

Since the aim of the present study was not an absolute evaluation, but a comparison of the surface performances of different gear steels, the micropitting tests were conducted on discs.

Test apparatus

The surface performances of the most promising innovative material, the Jomasco steel, as well as of the base line material, the 18NiCrMo5 steel, were investigated on a disc-on-disc test rig. In this type of test rig, two test discs are pressed one against the other in order to generate the sought contact pressures between the active surfaces of the two discs. These discs are mounted on two parallel shafts as can be seen in the layout of the twin disc test rig shown in Figure 8. One shaft is connected to a support fixed to the test rig frame, while the other one to a mobile support actuated by a hydraulic linear actuator. The force exerted by this actuator is measured using a load cell and controlled by a closed-loop control system. The two shafts are individually driven by two independent timing belt transmission systems moved by an electric motor with a speed variable between 0 and 3000 r/min. Thus, the two discs can rotate in opposite directions and at different speeds, keeping fixed the ratio of their tangential velocities in the ideal point of contact. The test bench is also equipped with a controlled lubrication system for the test discs so that they can be spray lubricated with an adjustable lubricant flow rate using two orientable nozzles.

Concerning the macro geometry of test specimens, each pair of test discs was made up of two case hardened and ground discs with the same external diameter of 65 mm in the transverse cross section, while one had a flat profile and the other one had a circularly crowned profile with a radius of 65 mm in the meridian cross section. The main macro and micro geometric characteristics of a test disc pair are shown in Figure 9. The geometries of the disc active surfaces result in a so-called point contact condition, and the contact area is an ellipse with the major axis parallel to the rotation axes. This geometry was chosen in order to generate sufficiently high contact pressure with the available test apparatus and to be representative as much as possible of gear contacts. Concerning the micro geometry of test discs, they were circumferentially ground at the end of their manufacturing process so that a circumferentially oriented surface lay was generated, i.e. the surface roughness lay was not oriented as usual in ground gears with respect to rolling direction. The mean arithmetic surface roughness parameter, Ra, had a mean value over the measurements performed on all the tested discs equal to 1.10 μm in the axial direction.

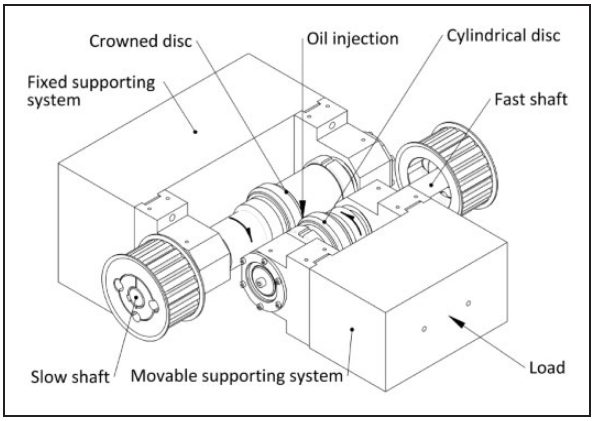

Figure 8. Layout of the twin disc test rig.

Test procedures

The tests were performed with a load stage procedure, i.e. by increasing stepwise the applied normal load up to 3 kN and, consequently, the maximum Hertzian contact pressure up to about 2 GPa. The load levels were chosen in order to obtain a constant increment of about 230 MPa between one load stage and the next one. The exact loading sequence of the test procedure adopted is shown in Figure 10. Each load stage was run for 8 h and 20 min corresponding to one million of load cycles for the fastest disc, i.e. the cylindrical one, apart from the running-in stage, i.e. the first load stage, that was run for 0.5 million load cycles at a reduced speed of 1500 r/min. After the running-in stage, all load stages were run at the same operating conditions. The rotational speed of the electric motor and the transmission ratios of the two belt systems were chosen so that the discs operated with a slide-to-roll ratio of 10% and a rolling velocity of 6.5 m/s, being the rotational speed of the fast shaft equal to 2000 r/min. In the tests, the discs were spray lubricated with an ISO VG 100 mineral oil injected on the ingoing side of the contact. This was a typical gear lubricant, commercially available under the trade name AGIP Blasia 100, formulated from paraffinic base stocks and additives such as phosphorous compounds, which ensure good low-speed and high-load performance.

These test conditions were chosen in order to obtain tribological conditions as close as possible to those generally found in industrial gear applications,

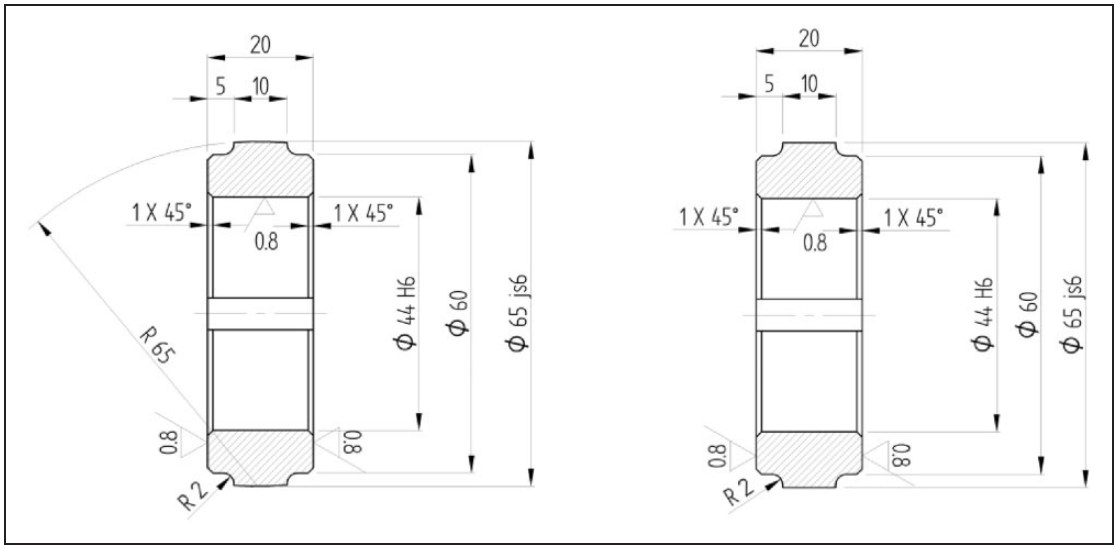

Figure 9. Longitudinal sections of the test discs. (a) Crowned disc, (b) cylindrical disc.

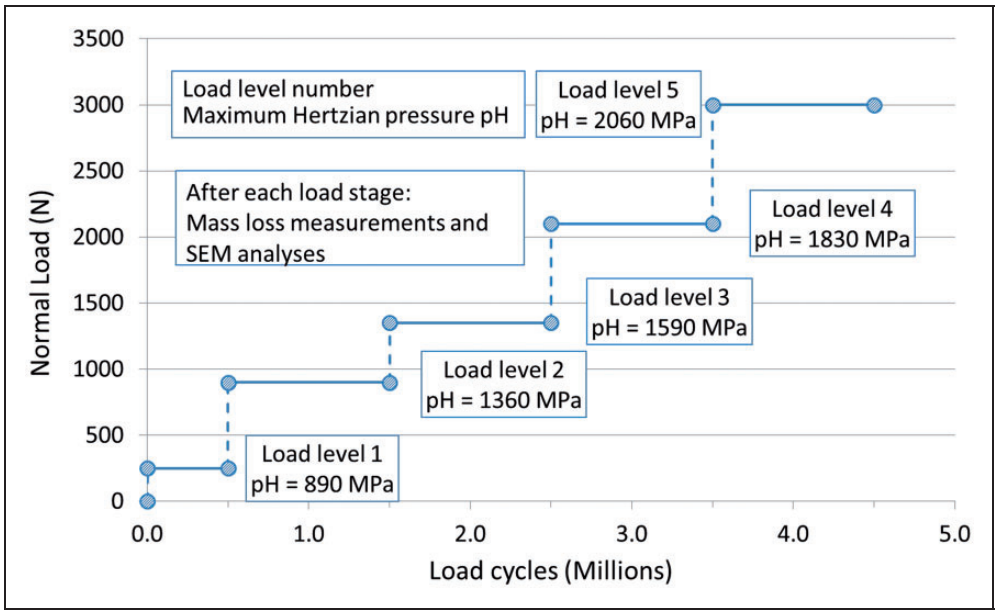

Figure 10. Micropitting test procedure – load stages.

but also able to promote micropitting damage on the active disc surfaces.

In order to analyse, quantify and document the micropitting damage evolution, at the end of each load stage the discs were dismounted, cleaned with white spirits in an ultrasonic bath and finally inspected by means of a SEM and weighted with a high precision scale determining the mass loss per each load stage.

In this load stage test, the contact fatigue strength of gear materials is determined in the form of a failure load stage under specific operating conditions (rolling and sliding velocities, lubricant and lubrication types, etc.). A failure criterion based on the mass loss per load stage has been adopted to identify the failure load stage and, thus, to determine a parameter that can be used to discriminate between the micropitting strength of the analysed gear materials. Of course in this kind of test, as well as in other type of gear material tests, e.g. pitting tests, the failure criterion is somehow arbitrary since the damage phenomenon does not result directly in a catastrophic and clearly identifiable failure as for example in bending fatigue tests. For this test the limit value of 8 mg per load stage was chosen as a failure condition.

Experimental test results

A synthesis of the micropitting test results is given in terms of diagrams in which the cumulative mass loss is plotted against the applied normal load. The results obtained for the two materials for both cylindrical

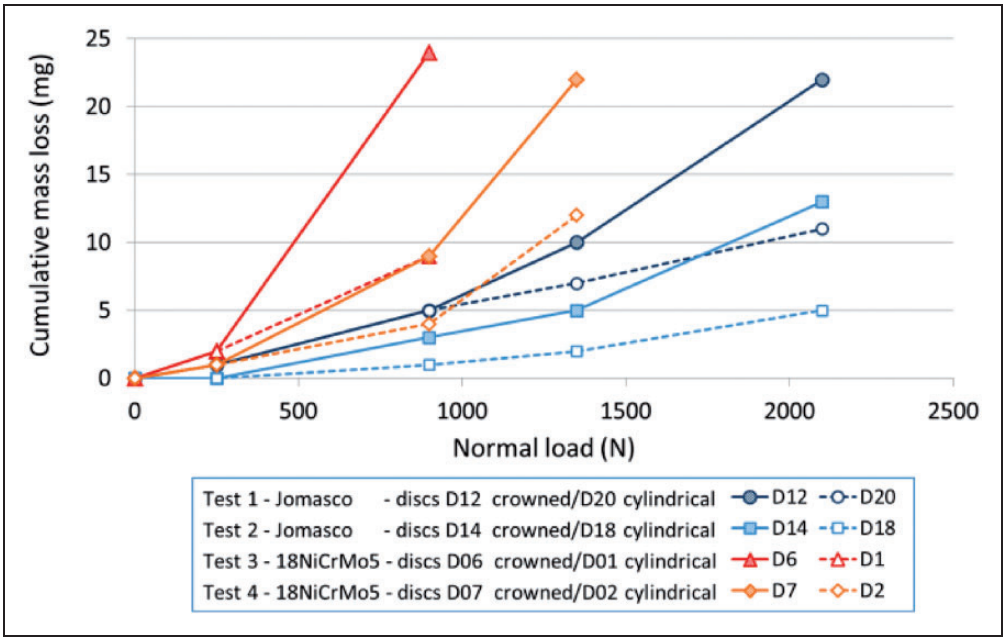

Figure 11. Results of micropitting tests in terms of cumulative mass loss versus applied load.

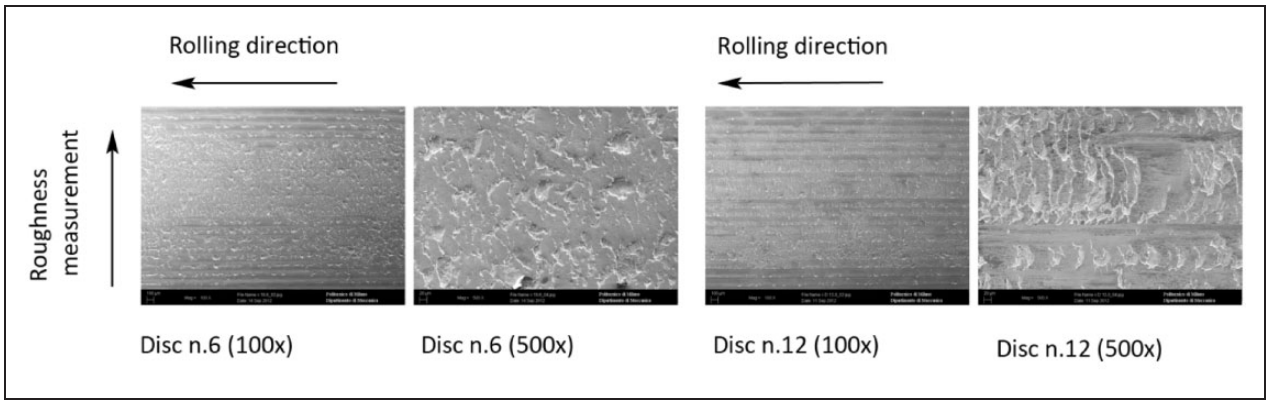

Figure 12. SEM images at different magnification (100 × and 500×) of the active surfaces of crowned discs 12 and 6 at the end of tests. (a) 18 NiCrMo5, (b) Jomasco.

and crowned discs are shown in Figure 11 and the damage appearance documented by SEM micrographs at the end of tests is shown in Figure 12. As can be seen from these diagrams, a weight loss occurred for both cylindrical and crowned discs for both the materials. This weight loss was the result of the surface damage occurred in the tests. To the naked eye, the damage appeared as a surface band with a frosted and light grey appearance that is typical of the micropitting damage, which for this reason is named also frosting or grey staining. Under a SEM, the damage was characterized by the typical features of rolling contact fatigue. On the active disc surfaces, there were many craters, micropits, typically only 5–10 μm deep and with a surface size of some 10 μm at the first occurrence. Surface cracks, which are the first step of micropit formation, were found as well by means of SEM inspections of the active surfaces. Therefore, the damage occurred during the tests can be surely classified as a rolling contact fatigue damage and, in particular, as micropitting.

In all the performed tests, the crowned discs, which operated in a negative sliding condition, showed a weight loss higher than the one observed for the cylindrical discs, which operated in a positive sliding condition. This experimental finding is in accordance with experiments conducted on gears in which micropitting damage is, generally, more severe on the dedendum flank of gears than on the addendum flank as observed, for example in Ref. 17. This fact is generally explained by the crack pressurization effect.[18] In a negative sliding condition, the tangential tractions on the contact surface due to friction open the surface cracks before the arrival of the contact load allowing the lubricant to flow into the crack and, subsequently, to be pressurized when the load passes over the crack promoting a mode I crack propagation. On the contrary, in a positive sliding condition, the surface

tractions due to their direction, coincident with one of the motion of the contact pressure distribution, close the surface cracks so that no oil can enter and, thus, no pressurization effects are possible.

Even if the number of the test points is limited and the results show some dispersion, the quantitative evaluation of the micropitting damage by means of mass loss measurements on crowned discs showed that the Jomasco steel had a micropitting strength higher than the one of the baseline material, the 18NiCrMo5 steel. In particular, taking into account the failure criterion chosen for this test campaign, both the Jomasco disc pairs failed at the fourth load level, while both the 18NiCrMo5 disc pairs failed at the second load level. This experimental finding confirms the suitability of the Jomasco steel as an alternative material to the widely used 18NiCrMo5. In any case these results have to be considered as preliminary and a more comprehensive activity of specific micropitting test on a back-to-back test rig has been programmed for the selected solution.

Conclusions

The bending fatigue limits of the materials tested during the present research provide useful data that can be used by gear designers for the rating of gearboxes. Instead, the contact fatigue tests do not provide data that can be used directly in the assessment of gears but, in any case enables a comparison of new materials with a traditional solution.

The results of bending and contact fatigue tests on two innovative gear materials presented in this paper, along with the studies on the heat treatment process and the manufacturing of a full-scale demonstrator, confirm that the Jomasco steel is suitable for the application to large size gears, as those used in wind turbine gearboxes. The use of this air-hardenable steel with low treatment distortion can significantly contribute to the cost-effectiveness and to the environmental sustainability of the manufacturing process chain of large gears.

Acknowledgements

The authors gratefully acknowledge the support given by the partners of the Research Project XL-Gear: Galbiati Group SpA, Flame Spray SpA, Colmegna SpA and D'Appolonia SpA.

Conflict of interest

None declared.

Funding

The research project XL-GEAR has been funded by Regione Lombardia – Programma Operativo Regionale 2007-2013 – Obiettivo 'Competitività regionale e occupazione' – Linea di intervento 1.1.1.1.A – Aree Tematiche Prioritarie 2009.

References

1. XL-Gear Consortium. Relazione Finale Progetto XL-Gear ID13690679. Report for the Regione Lombardia D.G. Industria, Artigianato, Edilizia e Cooperazione, December 2012, Milan, Italy.
2. Niemann G and Winter H. *Maschinenelemente, Band II, Getriebe allgemein, Zahnradgetriebe – Grundlagen, Stirnradgetriebe*. 2nd ed. Berlin: Springer-Verlag, 2002.
3. ISO 6336-5:2003. Calculation of load capacity of spur gears – Part 5: Strength and quality of materials.
4. Temmel C and Karlsson B. The bending fatigue strength of gears in isotropic 20NiMo10 steel in as-machined, single-peened and double-peened condition. *HTM J Heat Treatm Mat* 2011; 66: 24–29.
5. Temmel C, Karlsson B and Leicht V. Bending fatigue of gear teeth of conventional and isotropic steels. *HTM J Heat Treatm Mat* 2009; 64: 80–88.
6. Gasparini G, Mariani U, Gorla C, et al. Bending fatigue tests of helicopter case carburized gears: Influence of material, design and manufacturing parameters. In: *American Gear Manufacturers Association (AGMA) Fall Technical Meeting, 2008*, San Antonio Texas, USA, 12–14 October 2008. Paper no. 08FTM11. Red Hook, NY, USA: Curran & Associates Inc, pp.131–142.
7. Bian XX, Zhou G, Liwei, et al. Investigation of bending fatigue strength limit of alloy steel gear teeth. *Proc IMechE, Part C: J Mechanical Engineering Science* 2012; 226: 615–625.
8. Lemaitre C, Dierrickx P, Robat D, et al. Wear, base tooth fatigue and pitting tests on nitrided steels 25MnSiCrVB6/L (METASCO) and 23MnCrMo5-mod-1 (JOMASCO) – dimensional reliability, manufacturing savings and automotive filed applications. In: *IFHTSE-AIM 2nd international conference on heat treatment and surface engineering in automotive applications*, 20–22 June 2005, Riva del Garda, Italy. Milano, Italy: Associazione Italiana di Metallurgia (AIM).
9. SAE Standard J1619 1997-01-01. Single tooth gear bending fatigue test.
10. Krantz T and Tufts B. Pitting and bending fatigue evaluations of a new case-carburized gear steel. In: *ASME PTG* 2007, Las Vegas, Nevada, September 2007. DETC 2007-34090. New York, USA: ASME.
11. ISO 6336-3:2006. Calculation of load capacity of spur and helical gears – Part 3: calculation of tooth bending strength.
12. MAAG Gear Company Ltd. *Maag gear book: Calculation and practice of gears, gear drives toothed couplings and synchronous clutch couplings*. Zurich: Maag Gear Company Limited, 1990.
13. UNI 3964:1985, Prove meccaniche dei materiali metallici. Prove di fatica a temperatura ambiente. Principi generali.
14. ISO/TR 15144-1:2012 Calculation of micropitting load capacity of cylindrical spur and helical gears – Part 1: Introduction and basic principles.
15. Hohn B-R, Michaelis K and Doleshel A. Limitations of bench testing for gear lubricants. In: Totten GE, Wedeven LD, Dickey JR, et al. (eds) *Bench testing of industrial fluid lubrication and wear properties used in machinery applications*. West Conshohocken, PA, USA: ASTM International, 2001.

16. Gohritz A. *Ermittlung der Zahnflankentragfähigkeit mittler und großer Getribe durch Analogieversuche*. PhD Thesis, Aachen, 1982.
17. Hohn B-R, Oster P and Schrade U. Studies on the micropitting resistance of case-carburised gears – industrial application of the new calculation method. In: *Proceeding of the international conference on gears*, Garching, Germany, 14–16 September 2005, pp.1287–1307. VDI Berichte vol 1904.2. Düsseldorf, DE: VDI Verlag.
18. Bower AF. The influence of crack face friction and trapped fluid on surface initiated rolling contact fatigue cracks. *Trans ASME J Tribol* 1988; 110: 704–711.